

Measurement of hyperfine structure of sodium $3P_{1/2,3/2}$ states using optical spectroscopy

W.A. van Wijngaarden, J. Li

Department of Physics, York University, Toronto, Ontario, M3J 1P3 Canada
(Fax: +1-416/736-5516)

Received: 9 June 1994

Abstract. The hyperfine levels of the sodium $3P_{1/2,3/2}$ states were resolved using a narrow linewidth laser to excite the ground state. The laser frequency was scanned while fluorescence resulting from the radiative decay of the excited state was detected. The frequency was calibrated using the known hyperfine splitting of the ground state. The magnetic dipole A and electric quadrupole B hyperfine coupling constants of the excited states were determined to be $A_{3P_{1/2}} = 94.44 \pm 0.13$, $A_{3P_{3/2}} = 18.62 \pm 0.21$ and $B_{3P_{3/2}} = 2.11 \pm 0.52$ MHz. The uncertainty of $A_{3P_{1/2}}$ is less than results previously reported while the data for the $3P_{3/2}$ state are consistent with those existing in the literature.

PACS: 35.10.Fk

I. Introduction

Studies of the hyperfine interaction have provided increasingly accurate data to test atomic theory [1] and have found several unexpected phenomena such as the recent observation of hyperfine effects on the behaviour of ultra cold sodium atoms [2]. Extensive studies have been carried out on alkali-metal atoms [1, 3–5]. These atoms are especially simple to model since all but one electron occupies a filled electronic shell. Hence, the interaction between the valence electron and the nucleus surrounded by the electron core, can be approximated by a hydrogenic potential [6]. This model has been refined as a result of accurate measurements of the hyperfine interaction of excited states that revealed many body effects including core polarization and electron correlation [1]. Two years ago, interest in sodium was heightened by a discrepancy between the values of the ^{23}Na nuclear quadrupole moment obtained using atomic hyperfine measurements and muonic atoms [5, 7].

The Hamiltonian describing the hyperfine interaction is

$$H = Ah\mathbf{I} \cdot \mathbf{J} + Bh \frac{[3(\mathbf{I} \cdot \mathbf{J})^2 + \frac{3}{2}\mathbf{I} \cdot \mathbf{J} - (\mathbf{I} \cdot \mathbf{I})(\mathbf{J} \cdot \mathbf{J})]}{2I(2I-1)J(2J-1)} \quad (1)$$

where A and B are the magnetic dipole and electric quadrupole coupling constants and h is Planck's constant. \mathbf{I} is the nuclear spin and \mathbf{J} is the total electronic angular momentum. The eigenstates of the Hamiltonian are labelled by the total angular momentum $\mathbf{F} = \mathbf{J} + \mathbf{I}$ and have eigenenergy

$$E_F = \frac{1}{2} AhK + Bh \frac{3K(K+1) - 4I(I+1)J(J+1)}{8I(2I-1)J(2J-1)} \quad (2)$$

where $K = F(F+1) - I(I+1) - J(J+1)$. Table 1 lists the hyperfine energies for states having $J = 1/2, 3/2$.

The hyperfine interaction of alkali-metal atoms has been investigated using a variety of spectroscopic techniques which are nicely reviewed in the article by Arimondo et al. [3]. In the present work, a laser was scanned across the sodium D lines populating the various hyperfine levels shown in Fig. 1. The fluorescence produced by the radiative decay of the $3P_{1/2,3/2}$ states back to the ground state was then detected. The hyperfine splitting of the excited states was found using the ground state hyperfine splitting to calibrate the change in laser frequency. This method has the advantage of directly measuring the excited state hyperfine splitting and requires substantially simpler apparatus than other spectroscopic techniques. In this paper, the apparatus and procedure are described in Sect. II. The results are presented in

Table 1. Hyperfine energies

J	F	E_F
1/2	2	$0.75 A_{1/2}$
	1	$-1.25 A_{1/2}$
3/2	3	$2.25 A_{3/2} + 0.25 B_{3/2}$
	2	$-0.75 A_{3/2} - 0.75 B_{3/2}$
	1	$-2.75 A_{3/2} + 0.25 B_{3/2}$
	0	$-3.75 A_{3/2} + 1.25 B_{3/2}$

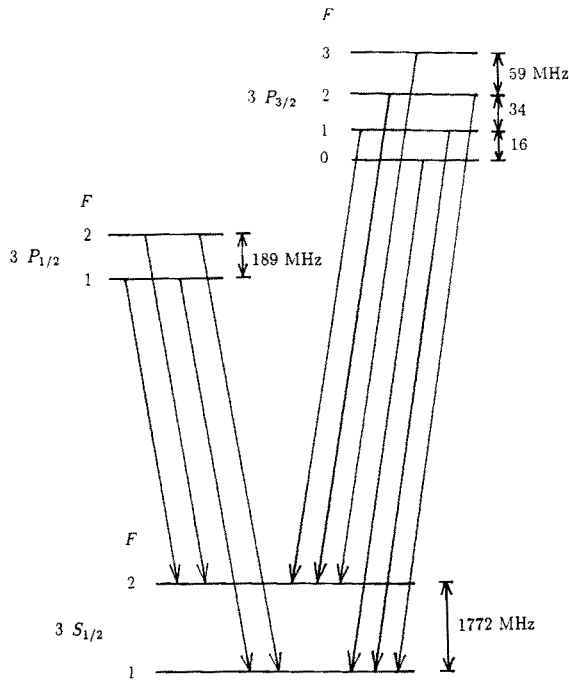


Fig. 1. Radiative transitions between hyperfine levels of the $3P_{1/2,3/2}$ and $3S_{1/2}$ states of ^{23}Na

Sect. III and compared with previous work. Finally, conclusions are made.

II. Apparatus and procedure

The apparatus is shown in Fig. 2. An oven was heated to about 300°C to produce an atomic beam. The sodium atoms were collimated by a series of slits resulting in a beam having a divergence of less than half a milliradian. The beam intensity was measured using a hot wire detector consisting of a hot filament that ionized the neutral atoms. The ion current was measured to be 0.5×10^{-9} amp. The oven and beam path were contained in a vacuum chamber that was pumped to a pressure of 1×10^{-7} torr using diffusion pumps and a liquid nitrogen trap.

The laser light was supplied by a ring dye laser (Coherent 699). This was pumped by an Argon ion laser (Innova 200) which produced 6 watts at a wavelength of 514 nm. A power of 150 milliwatts was obtained from the dye laser at the sodium D wavelength of 589 nm. The linewidth of the ring laser is specified by the manufacturer to be 0.5 MHz.

The resonances were found using a sodium vapor cell that was heated to about 100°C . The $3S_{1/2} \rightarrow 3P_{1/2,3/2}$ transition in the cell had a Doppler width of about 0.5 GHz which is much larger than the natural linewidth (9.7 MHz) obtained when exciting an atomic beam.

The laser intersected the atomic beam orthogonally to eliminate the first order Doppler shift. This was done using two 1 mm wide slits separated by 160 cm. The slits were located on either side of the vacuum chamber to which they were fastened. The intersection region of the

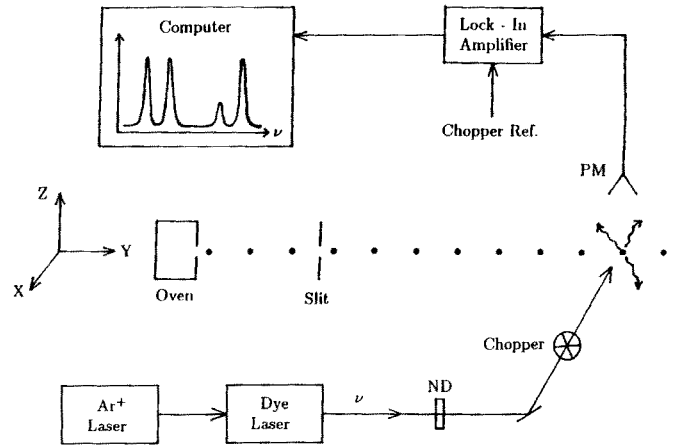


Fig. 2. Apparatus

laser and atomic beams was surrounded by three pairs of Helmholtz coils that cancelled the Earth's magnetic field which can shift the energy levels. The residual field was measured using a Hall effect gaussmeter (F.W. Bell 620) to be less than 10 milligauss. The fluorescence produced by the radiative decay of the $3P_{1/2,3/2}$ state back to the ground state was focussed by a lens having a focal length of 3.0 cm onto a photomultiplier (Hamamatsu R928). The interaction region of the laser and atomic beams was carefully shielded to reduce scattered light to a negligible amount.

The photomultiplier signal was sent to a lock-in amplifier (Stanford Research Systems 850). The reference signal was provided by a chopper that modulated the dye laser beam at a frequency of about 1.8 kHz. The lock-in digitized the signal at a rate of 256 Hz and stored it in a data file which was sent to a computer for analysis. A typical scan of the laser frequency across the hyperfine levels took a minute and produced a file consisting of 15 000 fluorescent intensity data points.

Typical data runs are shown in Figs. 3 and 4. The first two peaks in Fig. 3 arise from the excitation of the $3S_{1/2} F=2$ level to the $3P_{1/2} F=1, 2$ levels. Similarly the second pair of peaks is produced by exciting the $3S_{1/2} F=1$ level. In Fig. 5, the first set of three lines is produced by the transition of the $3S_{1/2} F=2$ level to the $3P_{3/2} F=1, 2, 3$ levels while the second set of three not completely resolved peaks results from exciting the $F=1$ ground state level to the $3P_{3/2} F=0, 1, 2$ levels. All data were taken using a series of neutral density filters (ND) to attenuate the laser power to about $1 \mu\text{watt}$. This was done to reduce the power broadening resulting in a maximum full width at half maximum fluorescent intensity of 12 MHz. This compares to the natural linewidth of 9.7 MHz obtained using the measured lifetime of the $3P_{1/2}$ state [9].

The location of the line center ν_0 was found by fitting a Lorentzian function

$$F(\nu) = \frac{F_0}{1 + \left(\frac{\nu - \nu_0}{\Gamma/2}\right)^2} \quad (3)$$

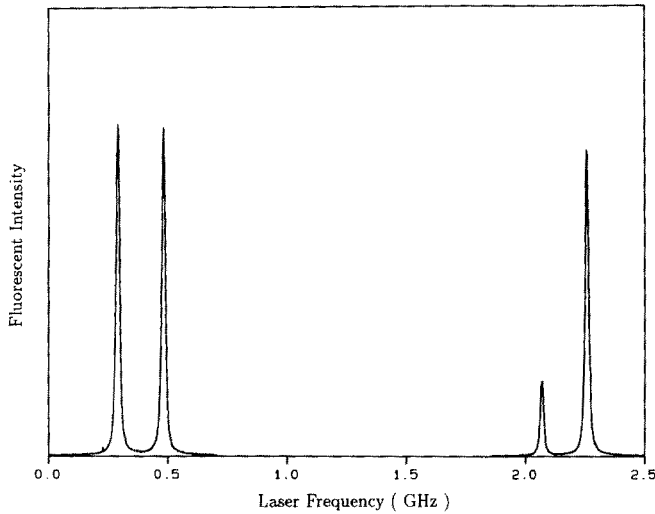


Fig. 3. Sample data of fluorescent intensity versus laser frequency. Data were taken while the laser excited the hyperfine levels of the $3P_{1/2}$ state

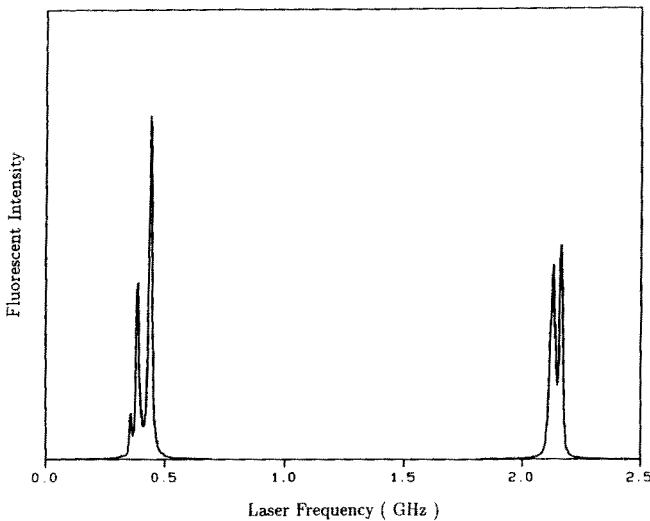


Fig. 4. Sample data of fluorescent intensity versus laser frequency. Data were taken while the laser excited the hyperfine levels of the $3P_{3/2}$ state

using a nonlinear least squares fit. Here, F_0 is the peak amplitude and F is the full width at half maximum intensity. For the first set of three peaks shown in Fig. 4 and shown magnified in Fig. 5, the data were fitted using three Lorentzian functions since the lines overlapped significantly. Figure 5 shows the curve that best fits the data.

The frequency axis was calibrated as follows. It is evident from Table 1, that the laser frequencies generating the first and third peaks as well as the second and fourth peaks in Fig. 3, differ by the ground state hyperfine splitting. This has been measured using the atomic beam magnetic resonance method to be 1771.62615(25) MHz [8]. This frequency was divided by the number of data points separating the line centers of the first and third peaks. This was repeated for the second and fourth peaks of Fig. 3 and the two results were averaged to find the fre-

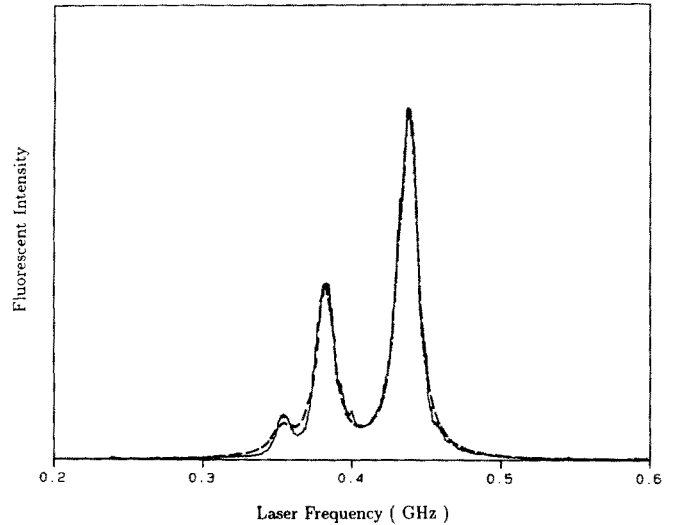


Fig. 5. Fit of fluorescence spectrum. The *solid line* is the fluorescent intensity measured when the laser excited the $3S_{1/2}F=2$ ground level to the $3P_{3/2}F=1, 2, 3$ levels. The *dashed line* is the fitted curve as is described in the text

quency interval represented by each data point. The frequency calibration for the D_2 line was done using the transitions from the $3S_{1/2}F=1, 2$ levels to the $3P_{3/2}F=2$ level which are also separated by the hyperfine splitting of the ground state. These transitions correspond to the second peak in Figs. 4 and 5 and the last peak in Fig. 4. The frequency axis of each scan was individually calibrated since the laser scan speed varied by up to 0.1% from one scan to the next. A typical value for the frequency interval represented by each point was 0.173 MHz.

The data gives the energy separations between the excited state hyperfine levels. The magnetic dipole and electric quadrupole coupling constants were obtained using the following relations which were derived using the energies listed in Table 1.

$$A_{3P_{1/2}} = \frac{E(F=2) - E(F=1)}{2} \quad (4)$$

$$A_{3P_{3/2}} = E(F=3) - \frac{E(F=1)}{5} \quad (5)$$

$$B_{3P_{3/2}} = (E(F=3) - E(F=2)) - \frac{3}{5}(E(F=3) - E(F=1)) \quad (6)$$

III. Results and conclusions

The averaged results for the hyperfine coupling constants along with the statistical uncertainties are listed in Table 2. Two hundred wavelength scans were taken to determine $A_{3P_{1/2}}$ while the results for the $3P_{3/2}$ state were found using 37 wavelength scans. Table 2 also lists the two results having the smallest quoted uncertainties found in the literature. References to other measurements can be found in the article by Yei et al. [5].

Table 2. Hyperfine constants of $3P_{1/2,3/2}$ states

State	A (MHz)	B (MHz)	Reference
$3P_{1/2}$	94.3 ± 0.2		[10]
	94.25 ± 0.15		[11]
	94.44 ± 0.13		This work
	91.7		Theory [1]
$3P_{3/2}$	18.64 ± 0.06	2.77 ± 0.06	[12]
	18.534 ± 0.015	2.724 ± 0.030	[5]
	18.62 ± 0.21	2.11 ± 0.52	This work
	18.49		Theory [1]

Hartmann [10] studied the $3P_{1/2}$ state using the optical double resonance method. A lamp excited sodium atoms contained in a vapor cell. The atoms were subjected to a magnetic field of about 2600 gauss that produced an energy splitting of the Zeeman sublevels. The frequency of magnetic dipole transitions between these levels was measured and used to determine the hyperfine constant $A_{3P_{1/2}}$.

Pesch et al. [11] used the technique of saturation spectroscopy. Two laser beams originating from the same dye laser were incident on a sodium cell. One laser beam saturated the $3S_{1/2} \rightarrow 3P_{1/2}$ transition while the transmission of the second lower power laser through the cell was measured. Hence, when the first laser excited a hyperfine level, a reduction in the absorption of the probe laser occurred. The dye laser was tuned across the D_1 line and the various hyperfine levels of the $3P_{1/2}$ state were detected with a fullwidth at half maximum signal of 20 MHz. The change in laser wavelength was initially monitored using a Fabry Perot etalon having a free spectral range of 150 MHz. This permitted the hyperfine splittings of the $3P_{1/2}$ state to be determined to within a few MHz. This uncertainty was caused by temperature fluctuations that affected the interferometer's optical length. An improved frequency calibration was carried out using two HeNe lasers and a different reference cavity. The dye laser was locked to the reference cavity which in turn was locked to a free running HeNe laser. The HeNe laser was frequency offset from a second HeNe laser whose frequency was lamb-dip stabilized to ± 50 kHz. The dye laser was tuned by varying the frequency offset of the two HeNe lasers which was measured using a frequency counter.

The $3P_{3/2}$ state has been studied by two groups using quantum beat spectroscopy [5, 12]. Krist et al. [12] generated an atomic beam by neutralizing a 150 keV Na^+ beam in a gas cell. A dye laser excited the atoms into a superposition of hyperfine levels of the $3P_{3/2}$ state. The temporal dependence of the radiative decay of the excited state back to the ground state was determined by measuring the fluorescent intensity along the beam path. The fluorescent signal varied from over 10^6 counts/sec where the laser beam excited the atoms, to 10^3 counts/sec when the detector position corresponded to the distance travelled by the atoms in 150 ns following the laser excitation. Eight quantum beat oscillations in the fluores-

cent signal were observed. This signal was then fitted to yield $A_{3P_{3/2}}$ and $B_{3P_{3/2}}$.

More accurate results for the $3P_{3/2}$ state have been reported by Yei et al. [5]. A pulsed dye laser excited sodium atoms contained in a cell. The hyperfine interaction then interchanged the populations of the excited state Zeeman sublevels. This was monitored by using a second pulsed laser to excite the $3P_{3/2}$ state to the $5S_{1/2}$ state which in turn decays to the $4P$ state. The fluorescence produced by the $4P \rightarrow 3S_{1/2}$ transition was then detected. The temporal evolution of the Zeeman sublevel populations was studied by varying the time delay between the excitation and probe laser pulses. This time delay was determined with an uncertainty of 0.02 ns by measuring the different pathlengths traversed by the two laser beams with a tape measure. The plot of fluorescence versus the time delay shows eight quantum beats during a time of about 130 ns. Each data point had a 2% uncertainty. The data were fitted yielding the hyperfine constants listed in Table 2. The fit contained a time offset parameter whose inclusion is stated to change the results for the hyperfine constants by about two standard deviations, even though its value was only -0.22 ns. It is not clear why more accurate results were obtained than those found by Krist et al. since the latter's data appear to have a higher signal to noise ratio.

The various experimental results found using different spectroscopic methods are in close agreement. However, the measured values are slightly larger than the computed magnetic dipole constants for both the $3P_{1/2,3/2}$ states [1], indicating the need for theoretical refinement. The theoretical values have been computed using many-body theory and take into account the polarization of inner core electrons as well as lowest order electron correlation effects.

In conclusion, we wish to emphasize the simplicity of the apparatus used here. Hyperfine structure can be examined without using several stabilized lasers and Fabry Perot etalons. Fast electronics needed for quantum beat spectroscopy are also not required. Furthermore, the data analysis is simpler since no assumptions about the state generated by the laser excitation or its evolution are necessary. Only the hyperfine splitting of the ground state is used to calibrate the laser frequency. If this quantity is not available or insufficiently accurate, one can modulate the laser using either an acousto-optic or electro-optic modulator [13]. Hence, a laser at frequency ν will acquire sidebands at frequency $\nu \pm \nu_{\text{mod}}$ where the modulation frequency ν_{mod} can be readily specified to a part in 10^6 using a frequency synthesizer. A laser scan across a transition then contains several fluorescent intensity peaks separated by ν_{mod} which can be used to calibrate the frequency. Hence, the method of examining excited state hyperfine structure by frequency scanning a laser across an atomic beam transition uses comparatively simple apparatus and yields results of high accuracy.

References

1. Lindgren, I., Lindgren, J., Martensson, A.: *Z. Phys.* **A279**, 113 (1976)
2. Wagshul, M.E., Helmerson, K., Lett, P.D., Rolston, S.L., Phillips, W.D., Heather, R., Julienne, P.S.: *Phys. Rev. Lett.* **70**, 2074 (1993)
3. Arimondo, E., Inguscio, M., Violino, P.: *Rev. Mod. Phys.* **49**, 31 (1977)
4. Windholz, L., Musso, M.: *Z. Phys.* **D27**, 229 (1993)
5. Yei, W., Sieradzan, A., Havey, M.D.: *Phys. Rev.* **A48**, 1909 (1993)
6. Bates, D.R., Damgaard, A.: *Philos. Trans. Roy. Soc. London* **242**, 101 (1949)
7. Sundholm, D., Olsen, J.: *Phys. Rev. Lett.* **68**, 927 (1992)
8. Ramsey, A.T., Anderson, L.W.: *J. Chem. Phys.* **43**, 191 (1965)
9. Gaupp, A., Kuske, P., Andra, H.J.: *Phys. Rev.* **A26**, 3351 (1982)
10. Hartmann, W.: *Z. Phys.* **240**, 323 (1970)
11. Pescht, K., Gerhardt, H., Matthias, E.: *Z. Phys.* **A281**, 199 (1977)
12. Krist, T., Kuske, P., Gaupp, A., Wittman, W., Andra, H.: *Phys. Lett.* **61A**, 94 (1977)
13. van Wijngaarden, W.A., Li, J.: *J. Opt. Soc. Am. B* accepted for publication (1994)